

## A wavelet fusion approach to the reconstruction of isotropic-resolution MR images from anisotropic orthogonal scans

I. Aganj<sup>1</sup>, C. Lenglet<sup>2</sup>, E. Yacoub<sup>2</sup>, G. Sapiro<sup>1</sup>, and N. Harel<sup>2</sup>

<sup>1</sup>Electrical Engineering, University of Minnesota, Minneapolis, MN, United States, <sup>2</sup>Center for Magnetic Resonance Research, University of Minnesota, United States

**Introduction:** Hardware, timing, and SNR considerations restrict the slice-selection and the in-plane resolutions differently, generally resulting in thicker acquisition slices and therefore anisotropic voxels. This non-uniform sampling can be problematic, especially in image segmentation and clinical examination, since the image will be missing high frequencies in the slice-selection direction. High-resolution MR volumes with isotropic voxels may still be acquired by decreasing the slice thickness, however, at the cost of requiring the subject to be motionless for a clinically unreasonably long time, hence increasing the risk of motion artifacts. This can be alleviated by dividing the acquisition into (two or) three separate scans, with thicker slices yet complementary resolutions, each containing a considerable proportion of the high frequencies, in two out of the three directions, missing in the other ones. Every scan will then have a shorter acquisition time and a lower chance of undergoing motion-related distortion. Misalignment between the three scans can be corrected by employing a variety of available registration techniques, and the high-resolution image is eventually reconstructed from the three scans. Different approaches to combining the three orthogonal scans have been proposed in the literature. Simply averaging the volumes, as done in (Goshtasby et al, *CMIG'96*; Tsougarakis et al, *Patent'09*, #7634119), introduces artificial blurring in the results. To avoid this, the authors of (Hamilton et al, *Radiology'94*; Herment et al, *MRM'03*; Hoge et al, *ICIP'03*; Roullot et al, *SP'04*) have suggested combining the images in the Fourier domain, by averaging the information coming from multiple scans, and zero padding where no information is present. The assumption of the missing information being zero, however, would be mathematically equivalent to presuming the point spread function (PSF) of the MR scanner to be the *sinc* function, which is different from the actual rectangular-window function often used in the literature. Other approaches to the reconstruction of such data include (Bai et al, *ISS'04*; Tamez-Peña et al, *SPIE'01*; Museth et al, *Visu'02*). In this work, we adopt a non-iterative wavelet-based approach, which takes into account the actual PSF of the MR scanner.

**Methods:** Wavelet fusion techniques are commonly used to combine multiple images into a single one retaining important features from each (see (Hill et al, *BMVC'02*) and the references within). The wavelet transform of an image (Daubechies, “Ten Lectures on Wavelets”, 1992) consists of different blocks, each containing either the low- or high-frequency information corresponding to a unique Cartesian dimension of the image. The simplest 3D wavelet transform of an MR image (with “XYZ” coordinates) has eight blocks, often noted as “LLL,” “LLH,” “LHL,” ..., “HHH,” where, for instance, LHH stands for the block containing low-, high-, and high-frequency information in the X, Y, and Z directions, respectively. Now suppose that the three orthogonal scans have voxel sizes of  $2 \times 1 \times 1$ ,  $1 \times 2 \times 1$ , and  $1 \times 1 \times 2$  mm<sup>3</sup>. Then we may assume that the wavelet transform of, e.g., the first scan has useful information in its four L## blocks, but virtually no information in its H## blocks (“#” represents both H and L). This is especially true when Haar wavelet functions are used (as in here), which are particularly consistent with the rectangular-window PSF of the MR scanner. Similarly, the informative blocks of the second and third volumes would be the four #L# and the four ##L blocks, respectively. Therefore, we proceed to reconstruct the high-resolution image (in the wavelet domain) by using as many informative blocks as available from the datasets. For example, the reconstructed LLL block will be the average of the LLL blocks of all the three scans, the LLH will be the average of the LLH blocks of the first two scans, and the LHH will be the LHH of the first scan. The HHH block is the only one missing in all the three scans, which we handle by zero-padding the reconstructed image. Performing an inverse wavelet transform will be the final step in making the high-resolution image with isotropic voxels. Since the wavelet transform is performed using the Fast Wavelet Transform algorithm with the complexity of  $O(N)$  ( $N$  being the number of voxels), the entire process is done quickly and at once, as opposed to the iterative methods proposed in (Bai et al, *ISS'04*; Tamez-Peña et al, *SPIE'01*).

**Results and discussion:** Three orthogonal Susceptibility-Weighted Imaging (SWI) datasets were acquired on a 7T MRI (Siemens Avanto) with voxel sizes of (Fig. 1a)  $0.4 \times 0.4 \times 0.8$  mm<sup>3</sup>, (Fig. 1b)  $0.8 \times 0.4 \times 0.4$ , and (Fig. 1c)  $0.4 \times 0.8 \times 0.4$ . In addition, a high-resolution ground truth dataset with isotropic voxels of the size  $0.4 \times 0.4 \times 0.4$  mm<sup>3</sup> (Fig. 1d) was acquired. The three orthogonal datasets were combined using both simple averaging (Fig. 1e) and the proposed wavelet fusion method (Fig. 1f). Haar wavelet functions were used to account for the rectangular-window PSF of the MR scanner in the slice-selection direction. Simply averaging the scans (Fig. 1e) results in artificial blurring, due to the fact that the same weight has been given to high frequencies of all images. On the other hand, the image reconstructed by the proposed method (Fig. 1f) is sharper and visually closer to the ground truth (Fig. 1d). To better appreciate the improvement of the proposed approach, we have generated isosurface rendering of vessels within the imaged volume (Fig. 2), from isotropic (yellow) and anisotropic (red) voxels. Note the clear deformations of the vessel reconstruction using anisotropic voxels, making isotropic voxels critical for accurate and non-deformed segmentation of brain structures.

**Acknowledgments:** This work was partly funded by NIH (grants R01 EB008645, R01 EB008432, P41 RR008079, and P30 NS057091), ONR, NGA, NSF, DARPA, ARO, and the University of Minnesota Institute for Translational Neuroscience.

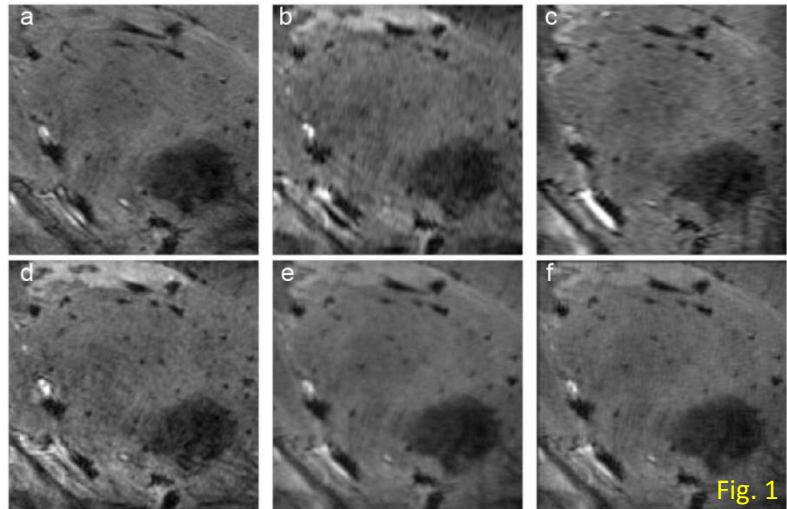


Fig. 1

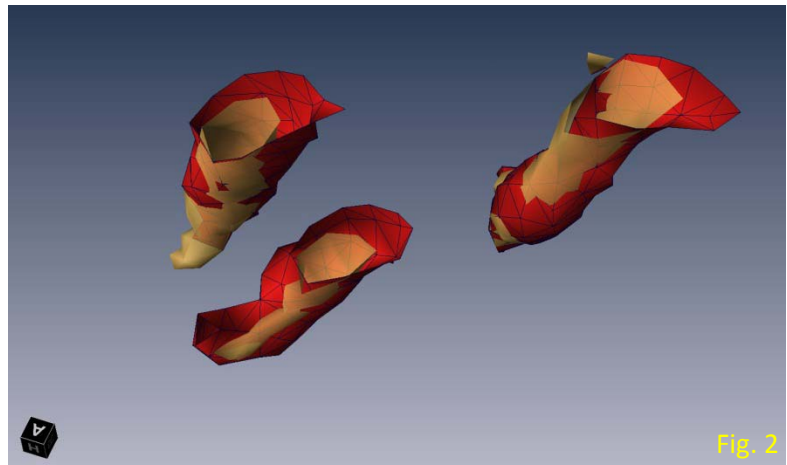


Fig. 2